

CoMFA and CoMSIA 3D-QSAR analysis on hydroxamic acid derivatives as urease inhibitors

ZAHEER-UL-HAQ, ABDUL WADOOD, & REAZ UDDIN

Dr. Panjwani Center for Molecular Medicine and Drug Research, International Center for Chemical & Biological Sciences, University of Karachi, Karachi-75270, Pakistan

(Received 11 October 2007; accepted 26 February 2008)

Abstract

Urease (EC 3.5.1.5) serves as a virulence factor in pathogens that are responsible for the development of many diseases in humans and animals. Urease allows soil microorganisms to use urea as a source of nitrogen and aid in the rapid break down of urea-based fertilizers resulting in phytotoxicity. It has been well established that hydroxamic acids are the potent inhibitors of urease activity. The 3D-QSAR studies on thirty five hydroxamic acid derivatives as known urease inhibitors were performed by Comparative Molecular Field Analysis (CoMFA) and Comparative Molecular Similarity Indices Analysis (CoMSIA) methods to determine the factors required for the activity of these compounds. The CoMFA model produced statistically significant results with cross-validated (q^2) 0.532 and conventional (r^2) correlation coefficients 0.969. The model indicated that the steric field (70.0%) has greater influence on hydroxamic acid inhibitors than the electrostatic field (30.0%). Furthermore, five different fields: steric, electrostatic, hydrophobic, H-bond donor and H-bond acceptor assumed to generate the CoMSIA model, which gave q^2 0.665 and r^2 0.976. This model showed that steric (43.0%), electrostatic (26.4%) and hydrophobic (20.3%) properties played a major role in urease inhibition. The analysis of CoMFA and CoMSIA contour maps provided insight into the possible modification of the hydroxamic acid derivatives for improved activity.

Keywords: Comparative molecular field analysis, comparative molecular similarity indices analysis, leave-one-out, hydroxamic acid, urease inhibitors

Introduction

The nickel containing enzyme, urease (urea amidohydrolases: E.C 3.5.1.5) catalyzes the rapid hydrolysis of urea to form ammonia and carbamate [1]. The spontaneous decomposition of carbamate yields a second molecule of ammonia and carbon dioxide. High concentration of ammonia arising from these reactions, as well as the accompanying pH elevation, has negative side effects in agriculture [2–4] and health [2,5,6]. For example, urease serves as a virulence factor in pathogens that are responsible for the development of kidney stones, pyelonephritis, peptic ulcers, and other medical complications [6]. The activity of soil-derived urease rapidly degrades urea-based fertilizers, causing significant environmental and economic problems by releasing large amount

of ammonia into the atmosphere during urea fertilization. This further contributes to phytotoxic effect and loss of volatilized nitrogen [7]. The enzyme also plays a critical role in the nitrogen metabolism of many microorganisms and plants [6,8]. Therefore, strategies based on urease inhibition are now seriously considered as the first line treatment for infections caused by urease-producing bacteria, to reduce environmental pollution and to enhance the efficiency of urea nitrogen uptake by plants.

Hydroxamic acid derivatives are highly potent and specific inhibitors of plant and bacterial urease activity [9,10]. Hydroxamic acid derivatives [R–CONH–OH, R–C(OH)=NOH] (HXA) characterized by a terminal hydroxyl amide (O=C–NHOH) functionality represent an important class of urease inhibitors. These inhibitors were reported by Kobashi et al.

Correspondence: Z. -Ul-Haq, Dr. Panjwani Center for Molecular Medicine and Drug Research, International Center for Chemical & Biological Sciences, University of Karachi, Karachi 75270, Pakistan. E-mail: zaheer_qasmi@hotmail.com. Fax: +9221 4819018-19.

in 1962. Since 1962 a wide range of hydroxamic acids have been designed and examined against urease of plant and microbial origin, including Jack bean (JB), *Clostridium sordelli*, *Escherichia coli*, *Morganella morganii*, *Proteus mirabilis* (PM), *Proteus vulgaris*, *Providencia rettgeri*, *Staphylococcus aureus* and *Bacillus pasteurii* (BP) [11–16].

In the present study, 3D-QSAR methods, CoMFA and CoMSIA, were applied to investigate the local physicochemical properties involved in the interaction between ligand and receptor. The widely used CoMFA (comparative molecular field analysis) calculates steric and electrostatic properties according to Lennard-Jones and Coulomb potentials [17]. The powerful CoMSIA approach (comparative molecular similarity indices analysis) calculates similarity indices in the space surrounding each of the aligned molecules in the data set [18–20]. CoMSIA is believed to be less affected by changes in molecular alignment and provides smooth and interpretable contour maps as result of employing Gaussian type distance dependence with the molecular similarity indices it uses [18]. The information provided by the derived 3D-QSAR models from hydroxamic acid derivatives can be used for designing and synthesis of potent urease inhibitors.

Computational methods

Data set and molecular structures

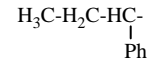
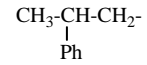
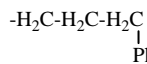
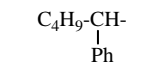
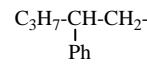
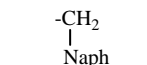
The 3D-structures and associated biological activities pIC_{50} ($\log 1/IC_{50}$) of thirty five compounds (Table I) were taken from the literature [21]. In the reported study Kobashi et al. investigated the correlation between the chemical structure and the inhibitory activities of hydroxamic acids and related compounds against sword bean urease. Seven out of thirty five compounds were randomly selected to form the external validation set while the remaining were used as training set for the construction of CoMFA and CoMSIA models.

The three dimensional structure of each ligand was modeled with the SYBYL 6.9 [22] molecular modeling program (Tripos Associates, Saint Louis, MO) using the sketch approach. The fragment libraries in SYBYL database were used as building blocks for the construction of larger ones. Each structure was first energy minimized using the standard Tripos force field [23] (Powell method and 0.05 Kcal/(molÅ) energy gradient convergence criteria) and electrostatic charges were calculated by the Gasteiger method [24] implemented in SYBYL, running on AMD Athelon desktop server using SuSe 9.1 operating system.

Alignment

The molecular alignment and orientation is one of the most sensitive input areas in 3D-QSAR studies. The accuracy of the prediction of a CoMFA model

Table I. Structure of the compounds 1–35 used for 3D-QSAR analyses.

R-CONHOH		
Compound	R	pIC_{50}
1	CH ₃ –	6.22
2	C ₂ H ₅ –	6.25
3	C ₅ H ₁₁ –	6.34
4	C ₆ H ₁₃ –	6.51
5	C ₇ H ₁₅ –	6.51
6	C ₈ H ₁₇ –	6.40
7	C ₉ H ₁₉ –	6.26
8	C ₁₀ H ₂₁ –	6.08
9	C ₁₁ H ₂₃ –	5.77
10	C ₁₃ H ₂₇ –	5.04
11*	C ₁₅ H ₃₁ –	4.68
12	<i>m</i> -Cl-Ph–	6.37
13	<i>m</i> -NO ₂ -Ph–	6.43
14*	<i>m</i> -CH ₃ -Ph–	6.20
15	<i>m</i> -CH ₃ O-Ph–	6.27
16*	<i>m</i> -C ₄ H ₉ O-Ph–	6.44
17	<i>m</i> -C ₆ H ₁₃ O-Ph–	6.15
18*	<i>m</i> -C ₈ H ₁₇ O-Ph–	6.44
19	Ph–	6.43
20	<i>p</i> -Cl-Ph–	6.52
21	<i>p</i> -NO ₂ -Ph–	6.43
22	<i>p</i> -CH ₃ -Ph–	5.96
23	<i>p</i> -OH-Ph–	6.37
24*	<i>p</i> -CH ₃ O-Ph–	6.64
25	<i>p</i> -C ₄ H ₉ O-Ph–	5.74
26	<i>p</i> -C ₆ H ₁₃ O-Ph–	5.64
27	<i>p</i> -C ₈ H ₁₇ O-Ph–	5.68
28	Ph-CH ₂ –	5.92
29	Ph-CH ₂ -CH ₂ –	6.70
30		4.96
31*		6.34
32		6.00
33		5.05
34*		5.92
35		5.07

* Test set compounds, $pIC_{50} = -\log IC_{50}$.

and the reliability of the contour maps strongly depend on the structural coordinates of molecules to be aligned according to reasonable bioactive conformations. In the present study the most active compound **29** was selected as a template and the remaining molecules were super-imposed on them by atom-fit option in SYBYL. The structure of compound **29** and the atoms used for alignment is shown in Figure 1 and the aligned molecules are shown in Figure 2.

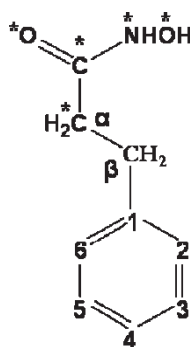


Figure 1. Structure of compound **29** used as a template on which all the compounds were superimposed using the atom-fit method; asterisks indicate the atoms selected for the fitting centers.

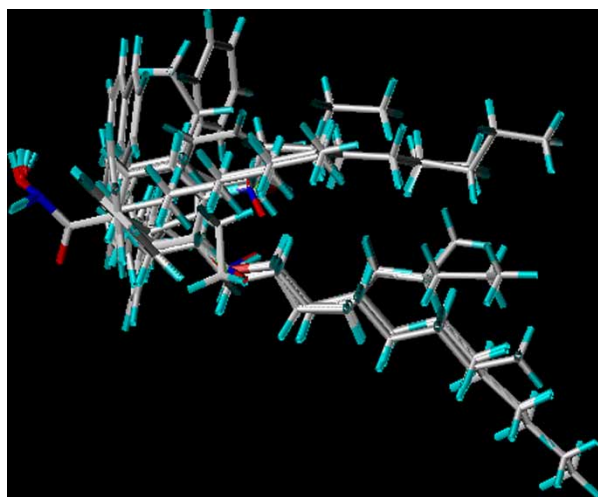


Figure 2. Alignment of compounds used to create the 3D-QSAR models.

CoMFA analysis

The aligned molecules (1–35) were placed in a three-dimensional grid (2 Å spacing) extending at least 2 Å beyond the volumes of all investigated molecules. The van der Waals potential and Coulombic terms representing the steric and electrostatic fields respectively were calculated using standard Tripos force field. A distance-dependent dielectric constant of 1.0 was used. An sp^3 carbon atom with +1.0 charges was used as a probe atom. The steric and electrostatic fields were truncated at ± 30.00 kcal/mol and the electrostatic fields were ignored at the lattice points with maximal steric interactions.

CoMSIA analysis

The molecular alignment was placed in a three-dimensional grid (2 Å spacing) similar to that of CoMFA analysis. CoMSIA differs from CoMFA in the implementation of the fields. It calculates steric and

electrostatic fields, in addition to hydrophobic, H-bond donor, and H-bond acceptor fields, and it used Gaussian values. CoMSIA has better ability to visualize and interpret the obtained correlations in terms of field contributions.

An sp^3 carbon was used as a probe atom with radius 1.0 Å and +1.0 charge with hydrophobicity of +1.0 and hydrogen bond donor and hydrogen bond acceptor properties of +1.0 was used to calculate steric, electrostatic, hydrophobic, hydrogen bond donor and acceptor fields.

Partial least square (PLS) analysis

CoMFA and CoMSIA descriptors were used as independent variables and pIC_{50} as the dependent variables in partial least squares (PLS) [25–27] regression analyses for the development of 3D-QSAR model, and cross-validation was performed using the leave-one-out method [28,29]. The cross-validated q^2 that resulted in optimum number of components and lowest standard error of prediction were considered for further analysis. Final analyses were performed to calculate conventional (non-cross-validated) r_{ncv}^2 using optimum number of components obtained from cross-validation procedure.

Results and discussion

Results of the CoMFA analysis

During the processes of model development and validation, we found that compound **28** did not fit to either training or test set compounds. This molecule was removed and further study was performed on the remaining 34 compounds. The results of CoMFA by PLS analysis derived from training set compounds are summarized in Table II which shows that a CoMFA model with a cross-validated q^2 of 0.532 for six components was obtained. The non-cross-validated PLS analysis with the optimum components of 6 ($N=6$) revealed a conventional r^2 value of 0.969, $F=103.996$, and an estimated standard error

Table II. Summary of CoMFA and CoMSIA results.

PLS statistics	CoMFA	CoMSIA
q^2	0.532	0.665
r^2	0.969	0.976
Standard Error of Estimate	0.117	0.103
F	103.996	135.69
Optimal component	06	06
Outlier	01	01
Field distribution (%)		
Steric	70.0%	43.0%
Electrostatic	30.0%	26.4%
Hydrophobic	–	20.3%
Hydrogen donor	–	6.2%
Hydrogen acceptor	–	4.2%

Table III. Actual and predicted inhibitory activities by CoMFA and CoMSIA analyses.

Compound	pIC ₅₀ activity	CoMFA prediction	CoMFA residual	CoMSIA prediction	CoMSIA residual
1	6.22	6.26	-0.04	6.23	-0.01
2	6.25	6.17	0.08	6.20	0.05
3	6.34	6.31	0.04	6.29	0.05
4	6.51	6.58	-0.07	6.59	-0.08
5	6.51	6.52	-0.01	6.54	-0.03
6	6.40	6.40	0.00	6.38	0.02
7	6.26	6.11	0.15	6.23	0.03
8	6.08	6.08	0.00	6.17	-0.09
9	5.77	5.65	0.09	5.69	0.08
10	5.04	5.02	0.02	5.05	-0.01
11*	4.68	5.04	-0.36	5.04	-0.36
12	6.37	6.43	-0.06	6.38	-0.01
13	6.43	6.33	0.10	6.41	0.02
14*	6.20	6.52	-0.32	6.50	-0.30
15	6.27	6.38	-0.11	6.38	-0.11
16*	6.44	6.41	0.03	6.35	0.09
17	6.15	6.11	0.04	6.12	0.03
18*	5.44	5.77	-0.33	5.89	-0.45
19	6.43	6.42	0.01	6.41	0.02
20	6.52	6.51	0.01	6.54	-0.02
21	6.43	6.45	-0.02	6.43	0.00
22	5.96	6.54	0.06	6.52	0.08
23	6.37	6.37	0.01	6.38	-0.01
24*	6.64	6.34	0.30	6.42	0.22
25	5.74	5.71	0.03	5.81	-0.07
26	5.64	5.38	0.26	5.34	0.30
27	4.68	4.94	-0.26	4.92	-0.23
28 outlier	5.92	5.51	0.41	4.90	1.02
29	6.70	6.82	-0.11	6.75	-0.04
30	4.96	5.12	-0.16	4.93	0.03
31*	6.34	6.37	-0.03	6.44	-0.10
32	6.00	6.13	-0.12	5.93	0.07
33	5.04	4.97	0.08	5.07	-0.01
34*	5.92	6.13	-0.21	6.14	-0.22
35	5.07	5.09	-0.02	5.12	-0.05

of 0.117. The steric field descriptors explain 70.0% of the variance, while the electrostatic descriptors explain 30.0%. These steric and electrostatic contribution results supported the previously published results [30] that the effect of electronic character of substituents have less contribution in inhibitory activities. The predicted activities, the experimental activities and their residual for the training and test sets compounds are listed in Table III. The table demonstrates that the predicted activities by the constructed CoMFA model are in good agreement with the experimental data, suggesting that the CoMFA model should have a satisfactory predictive ability.

Results of the CoMSIA analysis

The results of CoMSIA analysis for the training set molecules were presented in Table II. This model gave cross-validated correlation coefficient $q^2 = 0.665$ with 6 number of components ($N = 6$), a non-cross-validated r^2 of 0.976 with 43.0% steric, 26.4% electrostatic, 20.3% hydrophobic, 6.2% hydrogen bond donor and 4.2% hydrogen bond acceptor contributions. The actual inhibitory activities

(pCI₅₀), the calculated activities, predicted by the CoMSIA and their residuals for the training and test sets are given in Table III. These results demonstrate that the CoMSIA model also provide a good predictive value.

CoMFA contour maps

The QSAR produced by CoMFA, with its hundreds or thousands of terms, was usually represented as 3-D 'coefficient contour'. It shows regions where variations of steric or electrostatic nature in the structural features of different molecules contained in the training set lead to enhancement or reduction in the activity. The CoMFA contour plots of steric and electrostatic interaction are shown in Figure 3. The most active compound **29** was used in the background. Sterically favored (green) regions were found near C3 and C4 of phenyl ring and extending to the alpha-carbon of the reference compound where bulkier substituent may increase activity. Two sterically unfavorable (yellow) contours were found one above C6 of phenyl ring and the other away from the phenyl ring where the bulkier substituent may

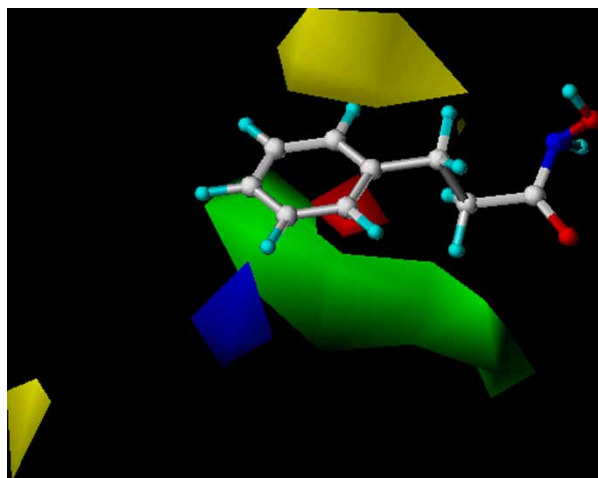


Figure 3. CoMFA contour plots for steric and electrostatic fields with compound **29** as a reference compound. Sterically favored areas are shown in green while the yellow isopleths depict sterically disfavored areas. Blue isopleths depict areas where positively charged groups increase activity and red areas indicate increase in the activity with negatively charged groups.

be detrimental to the activity. After visualizing each compound in the CoMFA contours it was observed that the green contours were present around the side chains of phenyl ring. It showed that the compounds containing sterically crowded substituents at this position will show higher activity than others. This observation is supported by the fact that the activities of compounds **1–11** are gradually increased as the steric crowdedness increased. But the activities increase to a certain limit because there is sterically unfavored yellow region just opposite the sterically favored green region. That is why the activity of compounds **8, 9, 10** and **11** are in the descending order. These sterically favored and unfavored CoMFA results are well consistent with the previous published results [21].

On the electrostatic contour maps (Figure 3) the negative charge favorable red region was found near the C1 of phenyl ring of the reference compound. This indicates that compounds containing electron donating groups at this position will show increased activity. This observation is well consistent with the experimental results, for example compound **2** having proton at this position showed less activity as compare to compounds **3, 4** and **5** which possess electron rich aliphatic chains at this position. These observations are in good agreement with previous published results [31,32], in which it is proved that electronegative groups that can interact favorably with nickel ions of the receptor, will be capable of effectively bind to the active site. One positive charge favored blue isopleths were found near *meta* position of phenyl ring of the reference compound. This observation is verified by the experimental results as the activity of compound **13** is greater than compound **14** because it contains electron donating group (nitro group) at this position.

CoMSIA contour maps

The steric contour maps from the CoMSIA analysis (Figure 4) are generally in accordance with the CoMFA steric maps (Figure 3). The contour maps of hydrophobic properties (Figure 5) indicate that hydrophobically favored (yellow) and disfavored (white) regions are around side chain in up and down positions. This observation is in agreement with CoMFA steric contour map (Figure 3), that shows the steric favorable green and unfavorable yellow regions at the same positions. On the electrostatic contour maps the negative charge favorable region (red) is very close to the CoMFA results. The positive charge favorable blue isopleths were found above alpha carbon of the reference compound. This observation is verified by the experimental results such as the activity of compound **28** is greater than compound **30** because in compound **28** the proton is attached to alpha carbon whereas in compound **30** the electron rich alkyl group is present at this position where negative charge is disfavored. This indicates that more positive charge is favored at this position which also support previously published results [33] in which benzohydroxamic acid at pH 5.0 shows more potent activity than at pH 8.0. This is because of the reason that at acidic pH 5.0 the benzohydroxamic acid is in a positively charged form. In the hydrogen bond donor and acceptor contour maps the hydrogen bond donor favorable (cyan) contour (Figure 6) was found near amido nitrogen and the hydrogen bond acceptor favorable (magenta) contour (Figure 7) was found near carbonyl oxygen of hydroxamic group in most of the compounds. These results highlight the importance of amido nitrogen and carbonyl oxygen as hydrogen bond donor and acceptor respectively. The hydrogen bond donor and acceptor disfavorable regions (purple and red) were observed near hydroxyl oxygen of hydroxamic group (Figures 6 and 7).

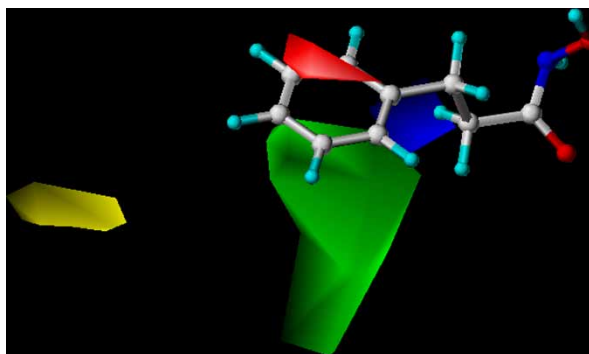


Figure 4. CoMSIA contour plots for steric and electrostatic fields with compound **29** as a reference compound. Sterically favored areas are shown in green while the yellow isopleths depict sterically disfavored areas. Blue isopleths depict areas where positively charged groups increase activity and red areas indicate increase in the activity with negatively charged groups.

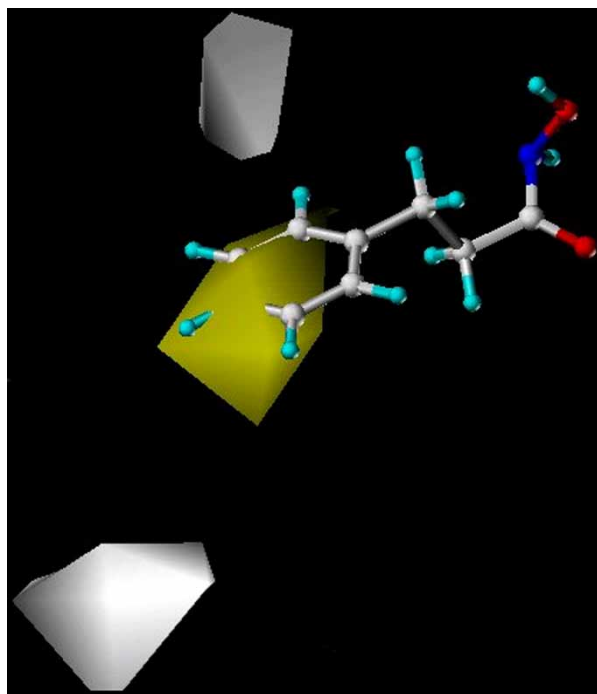


Figure 5. CoMSIA contour plots for hydrophobic interaction with compound 29 as a reference compound. Yellow regions indicate area where hydrophobic groups increase activity, and white regions indicate area where hydrophobic groups decrease activity.

This indicates that this hydroxyl group is equally important as a hydrogen bond donor and acceptor. These results of hydrogen bond donor and acceptor property are according to the published data [34] which further verified our 3D-QSAR models.

Conclusion

The 3D-QSAR analyses, CoMFA and CoMSIA were used to build statistically significant models with good correlative and predictive power for urease inhibitory

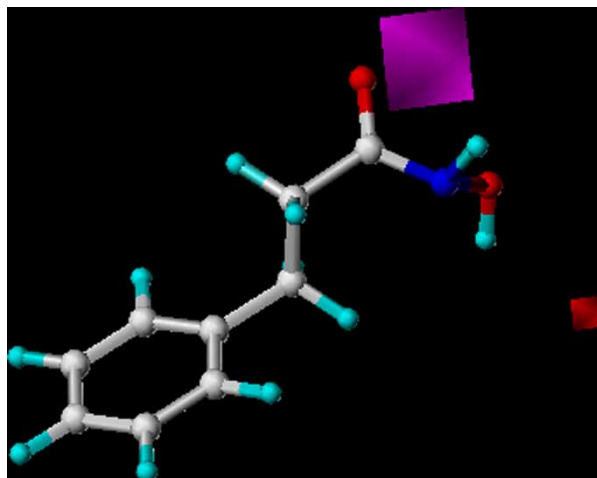


Figure 6. The predicted activities versus experimental activities (pIC_{50}) derived from the CoMFA model of the training set.

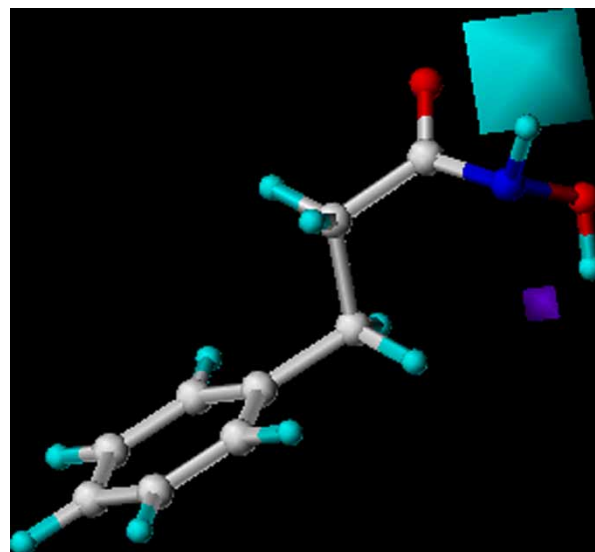


Figure 7. The predicted activities versus experimental activities (pIC_{50}) derived from the CoMSIA model of the training set.

activities of the hydroxamic acid derivatives. The robustness of the derived models was verified by the test set. Results of this study may provide an important basis for future drug design studies and synthesis of more potent urease inhibitors.

Acknowledgements

Financial support from Higher Education Commission, Pakistan under the establishment grant is highly acknowledged. We also greatly acknowledge the technical support provided by Professor Bernd M. Rode (University of Innsbruck) during this research.

Declaration of interest: The authors report no conflicts of interest. The authors alone are responsible for the content and writing of the paper.

References

- [1] Karplus PA, Pearson MA, Hausinger RP. *Acc Chem Res* 1997; 30:330–337.
- [2] Mobley HLT, Hausinger RP. *Microbiol Rev* 1989;53:85–108.
- [3] Bremner JM, Krogneier MJ. *Proc Natl Acad Sci USA* 1989;86: 8185–8188.
- [4] Bremner JM. *Fert Res* 1995;42:321–329.
- [5] Collins CM, D’Orazio SEF. *Mol Microbiol* 1993;9:907–913.
- [6] Mobley HLT, Island MD, Hausinger RP. *Science* 1995;59: 451–480.
- [7] Mulvaney RL, Bremner JM. *Soil Biochem* 1981;5:153–196.
- [8] Zonia LE, Stebbins NE, Polacco JC. *Plant Physiol* 1995;107: 1097–1103.
- [9] Kobashi K, Hase J, Uehara K. *Biochim Biophys Acta* 1962;65: 380–383.
- [10] Fishbein WN, Carbone PP, Hochstein HD. *Nature (London)* 1965;208:46–48.
- [11] Gale GC, Atkins IM. *Arch Int Pharmacodyn Ther* 1969;180:289–298, b) Kobashi K, Hase J, Uehara K. *Biochem Biophys Acta* 1962;62:380–383.
- [12] Hase J, Kobashi K. *J Biochem (Tokyo)* 1967;62:293–299.

- [13] Munakata K, Kobashi K, Takebe S, Hase J. *J Pharmacobiodyn* 1980;3:451–456.
- [14] Nervig RM, Kaidis S. *Can J Microbiol* 1976;22:544–554.
- [15] Rosenstein IJ, Hamilton-Miller JM, Brumfitt W. *Infect Immune* 1981;32:32–37.
- [16] a) Blakeley RL, Webb EC, Zerner B. *Biochemistry* 1969;8:1984–1990. b) Wu Z, Zhou X, Zhang W, Xu Z, You X, Haung XJ. *Chem Soc Chem Commun* 1994;7:813–814.
- [17] Cramer RD, III, Patterson DE, Bunce JD. *J Am Chem Soc* 1988;110:5959–5967.
- [18] Klebe G, Abraham U, Mietzner T. *J Med Chem* 1994;37:4130–4146.
- [19] Klebe G, Abraham U. *J Comput Aided Mol Des* 1999;13:1–10.
- [20] Büohm M, Stürzebecher J, Klebe G. *J Med Chem* 1999;42:458–477.
- [21] Kyoichi K, Kenji K, Junichi H. *Biochem Biophys Acta* 1971;227:429–441.
- [22] SYBYL 6.9 Tripos Inc., 1699 Hanley Road, St. Louis, MO 63144
- [23] Clark M, Cramer RD, III, van Opdenbosch N. *J Comp Chem* 1989;10:982–1012.
- [24] SYBYL, ver. 6.5., Tripos Associates: 1998 St. Louis, MO
- [25] Wold S, Albano C, Dunn WJ, Edlund U, Esbensen K, Geladi P, Hellberg S, Johansson E, Lindberg W, Sjöström M. *Chemometrics The Netherlands* 1984;:250–300.
- [26] Dunn WJ, Wold S, Edlund U, Hellberg S, Gasteiger J. *Quant Struct Act Relat* 1984;3:131–137.
- [27] Geladi P. *J Chemometrics* 1998;2:231–246.
- [28] Wold S. *Technometrics* 1978;20:397405.
- [29] Cramer RD, III, Bunce JD, Patterson DE. *Quant Struct Act Relat* 1988;7:18–25.
- [30] Kenji K, Suiichi T, Kyoichi K, Jun'ichi H. *Chem Pharm Bull* 1972;20:1599–1606.
- [31] Mishra H, Parrill AL, Williamson JS. *Antimicrob Agents Chemother* 2002;46:2913–2918.
- [32] Khan KM, Iqbal S, Lodhi MA, Maharvi GM, Ullah Z, Choudhary MI, Atta-ur-Rahman, Perveen S. *Bioorg Med Chem* 2004;12:1963–1968.
- [33] Ito Y, Onoda Y, Nadamura S, Tagawa K, Fukushima T, Sugawara Y, Takaiti O. *Jpn J Pharmacol* 1993;62:175–181.
- [34] Hpearson MA, Michel LO, Hausinger RP, Karplus PA. *Biochemistry* 1997;36:8164–8172.